arXiv:1002.4335v2 [cond-mat.supr-con] 27 Apr 2010

Constraints Imposed by Symmetry on Pairing Operators for the Pnictides

Xiaoyu Wang,[1, 2, 3] Maria Daghofer,[4, 1, 2] Andrew Nicholson,[1, 2]
Adriana Moreo,[1, 2] Michael Guidry,[1, 2] and Elbio Dagotto[1, 2]

[1] *Department of Physics and Astronomy, The University of Tennessee, Knoxville, TN 37996*
[2] *Materials Science and Technology Division, Oak Ridge National Laboratory, Oak Ridge, TN 32831*
[3] *Department of Electronic Communication and Engineering,*
Shanghai Jiao Tong University, Shanghai 200240
[4] *IFW Dresden, P.O. Box 27 01 16, D-01171 Dresden, Germany*

(Dated: April 28, 2010)

Considering model Hamiltonians that respect the symmetry properties of the pnictides, it is argued that pairing interactions that couple electrons at different orbitals with an orbital-dependent pairing strength inevitably lead to interband pairing matrix elements, at least in some regions of the Brillouin zone. Such interband pairing has not been considered of relevance in multiorbital systems in previous investigations. It is also observed that if, instead, a purely intraband pairing interaction is postulated, this requires that the pairing operator has the form $\Delta^\dagger(\mathbf{k}) = f(\mathbf{k}) \sum_\alpha d^\dagger_{\mathbf{k},\alpha,\uparrow} d^\dagger_{-\mathbf{k},\alpha,\downarrow}$ where α labels the orbitals considered in the model and $f(\mathbf{k})$ arises from the spatial location of the coupled electrons or holes. This means that the gaps at two different Fermi surfaces involving momenta $\mathbf{k}_F$ and $\mathbf{k}'_F$ can only differ by the ratio $f(\mathbf{k}_F)/f(\mathbf{k}'_F)$ and that electrons in different orbitals must be subject to the same pairing attraction, thus requiring fine tuning. These results suggest that previously neglected interband pairing tendencies could actually be of relevance in a microscopic description of the pairing mechanism in the pnictides.

PACS numbers: 75.50.Pp, 71.10.Fd, 72.25.Dc

I. INTRODUCTION

The discovery of superconductivity in the iron-based pnictides[1–8] has opened a new active direction of research in the quest to understand high critical temperature (high-T_c) superconductors. Experiments are showing that the pnictides share several properties with the high-T_c cuprates, such as the order of magnitude of the critical temperature,[1] the existence of magnetic order in some of the parent compounds,[9–13] and a possible exotic pairing mechanism.[14] However, there are differences in several aspects as well: the parent compound is a (bad) metal instead of a Mott insulator,[9–13] and several orbitals, as opposed to only one, have to be considered in order to reproduce the Fermi surface, which consists of hole and electron pockets.[15–18] In addition, while clear experimental evidence and theoretical calculations indicate that the pairing state in the cuprates is nodal and has d-wave symmetry,[19] the properties of the pairing operator in the pnictides have not yet been established. Experimentally, several angle resolved photoemission (ARPES) studies[20–25] show constant nodeless gaps on all Fermi surfaces (FSs), but evidence for the existence of nodal gaps has been reported in many transport measurements as well.[26–36] It has been argued that the properties of the gap may be material dependent or that a nodal gap may be rendered nodeless by disorder,[37] but a consensus has not been reached.

The goal of this paper is to understand the constraints that symmetries and the number of active degrees of freedom in the pnictides impose on the possible pairing operators. We will consider a *five* orbital model that retains the five d orbitals of each of the two Fe atoms in the unit cell of the FeAs planes.[38] Employing mean-field approximations we will discuss comparisons with results obtained in models with three[39] and two[40–42] orbitals that can be studied numerically.

The organization of the paper is as follows: in Section II we present the five-orbital Hamiltonian written in terms of SU(5) 5×5 matrices to properly identify its symmetries. The pairing operators are explicitly discussed in Section III. Section IV is devoted to a discussion of the results, while conclusions are provided in Section V.

II. MODEL

To construct the possible pairing operators allowed by the lattice and orbital symmetries, we will follow the approach already described in detail for the case of a three-orbital model.[39] The first step involves the rewriting of the tight-binding Hamiltonian for the five-orbital model, for instance as provided in Ref. 38, in terms of some of the 25 5×5 matrix generators of $U(5) \supset U(1) \times SU(5)$, which consist of the unit 5×5 matrix and 24 5×5 matrix generators of $SU(4)$. Since most of the elements of these matrices are zero, instead of providing for the reader this large number of matrices explicitly, it is more convenient to simply describe them verbally. For $i = 1$ up to 8, the λ_i matrices are given by the well-known eight Gell-Mann matrices[39] in the upper left-hand corner while the rest of the elements are equal to zero. The matrices with $i = 9$ $(1, 4)$, 11 $(1, 5)$, 13 $(2, 4)$, 15 $(2, 5)$, 17 $(3, 4)$, 19 $(3, 5)$, and 21 $(4, 5)$ are symmetric and have only two elements equal to 1 while the rest of the elements are 0, with (i, j) indicating the position of one of the non-zero elements (by symmetry the other element can be identified). The matrices with $i = 10$ $(1,4)$, 12 $(1,5)$, 14 $(2,4)$, 16 $(2,5)$, 18 $(3,4)$, 20 $(3,5)$, and 22 $(4,5)$ are Hermitian and have two elements equal to $\pm i$ and the rest are 0, with (i,j) indicating the position of the non-zero element equal to $-i$. Finally, λ_{23} is diagonal with nonzero elements (4,4) and (5,5) equal to 1 and -1, and λ_{24} is diagonal with nonzero elements $(1,1) = (2,2) = (3,3) = \frac{2}{\sqrt{15}}$, $(4,4) = \frac{-3}{\sqrt{15}}$ and $(5,5) = \frac{-1}{\sqrt{15}}$.

The Hamiltonian then becomes

$$H_{\mathrm{TB}}(\mathbf{k}) = \sum_{\mathbf{k},\sigma} \Phi^{\dagger}_{\mathbf{k},\sigma} \zeta_{\mathbf{k}} \Phi_{\mathbf{k},\sigma}, \tag{1}$$

where $\Phi^{\dagger}_{\mathbf{k},\sigma} = (d^{\dagger}_1(\mathbf{k}), d^{\dagger}_2(\mathbf{k}), d^{\dagger}_3(\mathbf{k}), d^{\dagger}_4(\mathbf{k}), d^{\dagger}_5(\mathbf{k}))_{\sigma}$ and

$$\zeta_{\mathbf{k}} = \sum_{i=0}^{24} a_i \lambda_i, \tag{2}$$

where the coefficients a_i are presented in Table I. The functions ξ_{ij} appearing in this Table are provided in the Appendix. The on-site energies for each orbital are given by $\epsilon_1 = \epsilon_2 = 0.13$ eV, $\epsilon_3 = -0.22$ eV, $\epsilon_4 = 0.3$ eV, and $\epsilon_5 = -0.211$ eV.[38] In addition, $e_i = \xi_{ii} + \epsilon_i$, and the chemical potential is 0. The index-to-orbital correspondence is the following: (1) xz, (2) yz, (3) $x^2 - y^2$, (4) xy, and (5) $3z^2 - r^2$.[38]

The symmetry operations that leave invariant the Fe-As planes can be mapped on the elements of the point group $D_{4\mathrm{h}}$[43,44] and, thus, the Hamiltonian has to remain invariant under all the operations of this group, which means that it must transform according to the irreducible representation $A_{1\mathrm{g}}$. This allows us to assign an irreducible representation to each of the λ_i matrices and, thus, classify possible pairing operators according to their symmetry.[39,45] It is important to realize that due to the strong hybridization among the orbitals, evident in all the terms in Eq. 1 where ξ_{ij} with $i \neq j$ appear, a proper characterization of the pairing operators by symmetry cannot be accomplished using only the band representation.

TABLE I: Coefficients for the λ_i matrices in Eq. 2 and the irreducible representation of $D_{4\mathrm{h}}$ according to which they transform. The ξ_{ij} are provided in the Appendix.

i	a_i	IR
0	$\frac{\sum_i e_i}{5}$	$A_{1\mathrm{g}}$
1	ξ_{12}	$B_{2\mathrm{g}}$
2	0	
3	$\frac{e_1 - e_2}{2}$	$B_{1\mathrm{g}}$
4	0	
5	$i\xi_{13}$	E_{g}
6	0	
7	$i\xi_{23}$	E_{g}
8	$\frac{e_1 + e_2 - 2e_3}{2\sqrt{3}}$	$A_{1\mathrm{g}}$
9	0	
10	$i\xi_{14}$	E_{g}
11	0	
12	$i\xi_{15}$	E_{g}
13	0	
14	$i\xi_{24}$	E_{g}
15	0	
16	$i\xi_{25}$	E_{g}
17	ξ_{34}	$A_{2\mathrm{g}}$
18	0	
19	ξ_{35}	$B_{1\mathrm{g}}$
20	0	
21	ξ_{45}	$B_{2\mathrm{g}}$
22	0	
23	$\frac{e_4 - e_5}{2}$	$A_{1\mathrm{g}}$
24	$\frac{\sqrt{15}}{5}\left(\frac{e_1+e_2+e_3}{3} - \frac{e_4+e_5}{2}\right)$	$A_{1\mathrm{g}}$

III. PAIRING OPERATORS

In order to construct the allowed pairing operators in multiorbital models the symmetries of the spatial, spin, and orbital contributions needs to be considered. Ignoring the orbital symmetry may lead to problems similar to those encountered in the early days of the study of magnetism when the spin contribution to the electronic wave functions was not included. Note that from the point of view of the orbital symmetry some of the previous efforts on superconductivity in multiorbital systems, such as in Ref. 46, are effectively dealing with non-hybridized "s-orbitals". Thus, those results cannot be straightforwardly applied to a system with strongly hybridized non-s orbitals. In fact, it was observed that the general form of a spin-singlet pairing operator in this case is given by[47]

$$\Delta^{\dagger}(\mathbf{k}) = f_i(\mathbf{k}) (\lambda_i)_{\alpha,\beta} (d^{\dagger}_{\mathbf{k},\alpha,\uparrow} d^{\dagger}_{-\mathbf{k},\beta,\downarrow} - d^{\dagger}_{\mathbf{k},\beta,\uparrow} d^{\dagger}_{-\mathbf{k},\alpha,\downarrow}), \tag{3}$$

where a sum over repeated indices α and β is implied; the operators d have been defined above, and $f(\mathbf{k})$ is the form factor that transforms according to one of the irreducible representations of the crystal's symmetry group.[39] The form factors that will be considered in this work and their corresponding irreducible representations of $D_{4\mathrm{h}}$ (according to which they transform) are presented in Table II. The index i in Eq. (3)indicates that different form factors may be needed if matrices λ_i with different symmetries are combined.

As in the case of the two[45] and three[39] orbital models, the properties of the pairing operators can be studied under a mean-field approximation. We need to remember that the five-orbital model is defined in terms of a pseudocrystal momentum $\mathbf{k}$ in an extended Brillouin zone.[38] In terms of the real momentum, the unit cell of the Fe-As planes contains two Fe ions and, thus, the band structure is composed of 10 bands in the reduced, or folded, Brillouin zone (BZ). This can be observed in Fig. 1(a) where the spectral function $A(\mathbf{k},\omega)$ is shown for the non-

TABLE II: Form factors $f(\mathbf{k})$ for pairs up to distance (1,1) classified according to their symmetry under $D_{4\mathrm{h}}$ operations.

#	$f(\mathbf{k})$	IR
1	1	$A_{1\mathrm{g}}$
2	$\cos(k_x)+\cos(k_y)$	$A_{1\mathrm{g}}$
3	$\cos(k_x)\cos(k_y)$	$A_{1\mathrm{g}}$
4	$\cos(k_x)-\cos(k_y)$	$B_{1\mathrm{g}}$
5	$\sin(k_x)\sin(k_y)$	$B_{2\mathrm{g}}$
6	$(\sin(k_x),\sin(k_y))$	E_{g}
7	$(\sin(k_x)\cos(k_y),\sin(k_y)\cos(k_x))$	E_{g}

interacting case along high symmetry directions in the folded BZ where the 10 bands are clearly seen. Thus, for each real momentum $\mathbf{q}$ there are 10 bands. Five of them are the bands of the five-orbital model for the pseudocrystal momentum $\mathbf{k}=\mathbf{q}$ and the other five are obtained from the same model by setting the pseudocrystal momentum to $\mathbf{k}=\mathbf{q}+\mathbf{Q}$, where $\mathbf{Q}=(\pi,\pi)$. Since in terms of the real momentum, the basis of the five-orbital model is expanded by states with momentum $\mathbf{q}$ for orbitals xz and yz and momentum $\mathbf{q}+\mathbf{Q}$ for the other three orbitals, this fact needs to be taken into account when pairing operators are being constructed. If only intraorbital pairing operators are considered it is sufficient to build a 10×10 Bogoliuvov-deGennes (BdG) matrix, but for interorbital pairing between electrons in orbitals 1, 2 with electrons in orbitals 3, 4, or 5, it is necessary to construct a 20×20 BdG matrix since the 10×10 matrix only allows to consider intraorbital pairs with pseudocrystal momentum $\mathbf{Q}$ rather than 0.[48]

The 10×10 BdG Hamiltonian is given by:

$$H_{\mathrm{BdG}}=\sum_{\mathbf{k}}\Psi^{\dagger}_{\mathbf{k}}H^{\mathrm{MF}}_{\mathbf{k}}\Psi_{\mathbf{k}}, \qquad (4)$$

with the definitions

$$\Psi^{\dagger}_{\mathbf{k}}=(d^{\dagger}_{\mathbf{k},1,\uparrow},d^{\dagger}_{\mathbf{k},2,\uparrow},d^{\dagger}_{\mathbf{k},3,\uparrow},d^{\dagger}_{\mathbf{k},4,\uparrow},d^{\dagger}_{\mathbf{k},5,\uparrow},$$
$$d_{-\mathbf{k},1,\downarrow},d_{-\mathbf{k},2,\downarrow},d_{-\mathbf{k},3,\downarrow}d_{-\mathbf{k},4,\downarrow},d_{-\mathbf{k},5,\downarrow}), \qquad (5)$$

and

$$H^{\mathrm{MF}}_{\mathbf{k}}=\begin{pmatrix} H_{\mathrm{TB}}(\mathbf{k}) & P(\mathbf{k}) \\ P^{\dagger}(\mathbf{k}) & -H_{\mathrm{TB}}(\mathbf{k}) \end{pmatrix}, \qquad (6)$$

where each element represents a 5×5 block with $H_{\mathrm{TB}}(\mathbf{k})$ given by Eq. (1) and

$$P(\mathbf{k})_{\alpha,\beta}=Vf(\mathbf{k})(\lambda_i)_{\alpha,\beta}, \qquad (7)$$

where $V=V_0\Delta$ is determined by the product of an unknown pairing strength V_0 and a parameter Δ that arises from minimizing the mean-field equations, as already explained in previous literature.[47]

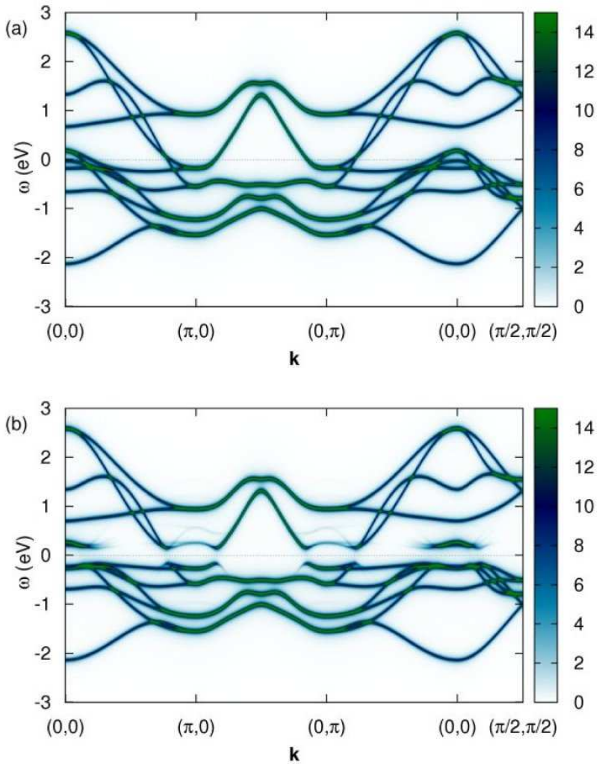

FIG. 1: (Color online) The intensity of the points represents the values of the spectral function $A(\mathbf{k},\omega)$ for the five-orbital model with pairing interaction (a) $V=0$; (b) $V=0.2$, and for the $S\pm$ pairing operator given in the text. The results are shown in the reduced BZ.

A. Intraorbital Pairing Operators

1. *Purely Intraband Pairing Operators*

The first issue we want to address is what is the form of the pairing operators resulting from purely intraband pairing interactions. The motivation is given by the fact that in standard BCS theory, the pairing occurs between particles with momentum equal in magnitude but opposite direction at a *common* Fermi surface. For this reason, even in multiorbital systems, it has been expected that pairing attraction should involve particles in the same band.[46] To determine whether a pairing operator consists of purely intraband matrix elements, we need to transform Eq. 6 from the orbital to the band representation in which H_{TB} is diagonal. The transformation is given by $H_{\mathrm{Band}}(\mathbf{k})=U^{\dagger}(\mathbf{k})H_{\mathrm{TB}}(\mathbf{k})U(\mathbf{k})$, where $U(\mathbf{k})$ is the unitary change of basis matrix and $U^{\dagger}(\mathbf{k})$ is the transpose conjugate of $U(\mathbf{k})$. Since U is unitary, for each value of $\mathbf{k}$, $\sum_i(U_{i,j})^*U_{i,m}=\sum_i(U_{j,i})^*U_{m,i}=\delta_{j,m}$. Then, $H'_{\mathrm{MF}}=G^{\dagger}H_{\mathrm{MF}}G$ where G is the 10×10 unitary matrix composed of two 5×5 blocks given by U. Then,

$$H'^{\rm MF}_{\mathbf{k}} = \begin{pmatrix} H_{\rm Band}(\mathbf{k}) & P_{\rm B}(\mathbf{k}) \\ P^{\dagger}_{\rm B}(\mathbf{k}) & -H_{\rm Band}(\mathbf{k}) \end{pmatrix}, \tag{8}$$

with

$$P_{\rm B}(\mathbf{k}) = U^{-1}(\mathbf{k}) P(\mathbf{k}) U(\mathbf{k}). \tag{9}$$

The most general form of a purely intraband pairing is given by

$$H'^{\rm MF}_{\mathbf{k}} = \begin{pmatrix}
\epsilon_1(\mathbf{k}) & 0 & 0 & 0 & 0 & \Delta_1(\mathbf{k}) & 0 & 0 & 0 & 0 \\
0 & \epsilon_2(\mathbf{k}) & 0 & 0 & 0 & 0 & \Delta_2(\mathbf{k}) & 0 & 0 & 0 \\
0 & 0 & \epsilon_3(\mathbf{k}) & 0 & 0 & 0 & 0 & \Delta_3(\mathbf{k}) & 0 & 0 \\
0 & 0 & 0 & \epsilon_4(\mathbf{k}) & 0 & 0 & 0 & 0 & \Delta_4(\mathbf{k}) & 0 \\
0 & 0 & 0 & 0 & \epsilon_5(\mathbf{k}) & 0 & 0 & 0 & 0 & \Delta_5(\mathbf{k}) \\
\Delta^*_1(\mathbf{k}) & 0 & 0 & 0 & 0 & -\epsilon_1(\mathbf{k}) & 0 & 0 & 0 & 0 \\
0 & \Delta^*_2(\mathbf{k}) & 0 & 0 & 0 & 0 & -\epsilon_2(\mathbf{k}) & 0 & 0 & 0 \\
0 & 0 & \Delta^*_3(\mathbf{k}) & 0 & 0 & 0 & 0 & -\epsilon_3(\mathbf{k}) & 0 & 0 \\
0 & 0 & 0 & \Delta^*_4(\mathbf{k}) & 0 & 0 & 0 & 0 & -\epsilon_4(\mathbf{k}) & 0 \\
0 & 0 & 0 & 0 & \Delta^*_5(\mathbf{k}) & 0 & 0 & 0 & 0 & -\epsilon_5(\mathbf{k})
\end{pmatrix}, \tag{10}$$

where $\epsilon_j(\mathbf{k})$ are the eigenvalues of $H_{\rm TB}(\mathbf{k})$, while $\Delta_j(\mathbf{k})$ denotes the band and momentum dependent pairing interactions. Notice that if $\lambda_i = \lambda_0$ in Eq.(7), $P(\mathbf{k})$ in Eq.(9) is proportional to the identity matrix and, thus, $P_{\rm B}(\mathbf{k})$ is diagonal with $\Delta_j(\mathbf{k}) = \Delta(\mathbf{k}) = Vf(\mathbf{k})$ for all j. This indicates that the *intraorbital* operator that pairs electrons in each orbital with *equal strength*, gives rise to a purely intraband pairing operator where electrons in each band are subject to an identical pairing attraction. In this case, diagonalizing Eq.(10) we obtain $E_j(\mathbf{k}) = \sqrt{\epsilon_j(\mathbf{k})^2 + |\Delta(\mathbf{k})|^2}$. Then, at $\mathbf{k}^j_F$ where $\epsilon_j(\mathbf{k}^j_F) = 0$ we obtain $E_j(\mathbf{k}^j_F) = |\Delta(\mathbf{k}^j_F)|$. This means that the superconducting gaps at the FS determined by different bands must satisfy that $\Delta'(\mathbf{k}'_F)/\Delta(\mathbf{k}_F) = \frac{f(\mathbf{k}'_F)}{f(\mathbf{k}_F)}$ where $\mathbf{k}'_F$ and $\mathbf{k}_F$ represent the Fermi momentum of two FS defined by two different bands. In the case of the standard low-temperature BCS pairing $f(\mathbf{k}) = 1$, implying that momentum independent gaps of equal magnitude should open in all the FSs. However, for the pnictides it is believed that a non-BCS interaction provides the source of pairing.[14] Then, we must consider the case in which $f(\mathbf{k}) \neq 1$. Notice that since λ_0 transforms according to A_{1g}, the symmetry of this purely intraband pairing operator is then totally determined by the symmetry of $f(\mathbf{k})$.

2. Single Gap: The $S\pm$ pairing operator

In the particular case in which $f(\mathbf{k}) = \cos k_x \cos k_y$, $P(\mathbf{k})$ transforms according to A_{1g} and it represents the simplest form of the well known $S\pm$ pairing state,[49–53] which will be characterized by gaps of approximately the same magnitude in the electron and hole pockets if there is good $(\pi, 0)$ and $(0, \pi)$ nesting. Note that the gap on the two hole FSs would differ only if they have considerably different Fermi momentum which is not the case in the pnictides since both hole pockets are very close to each other. In the five-orbital model we found that $r = \frac{f(\mathbf{k}')}{f(\mathbf{k})} \sim 1$ for the external hole and electron pockets, while $r \sim 0.9$ for the external and internal hole pockets. This means that the gaps in the two hole pockets would have a difference of only about 10%. The two Fermi surfaces would have to be much more separated from each other in order to develop the experimentally observed difference of 50% reported via ARPES experiments.[21]

In Fig. 2 we show the gap as a function of the angular position (from the x to the y axis) along the four Fermi surfaces (two electron and two hole pockets) for the five-orbital model in the folded BZ. Note that the values of the gap beyond $\Phi = \pi/4$ can be obtained by symmetry from the values shown in Fig. 2. The interaction $V = 0.02$ was chosen in order to obtain a quantitative match with experimentally reported values of the gaps that range between 1 to 20 meV.[25] As expected, it can be seen that the gaps at the external hole and electron pockets (dashed, continuous, and dotted lines) almost overlap with each other and have a magnitude of about 7 meV while at the internal hole pocket (dotted-dashed line) the gap is around 8 meV, i.e. only about 10% larger. Note that the momentum dependence observed here likely will be negligible when considering experimental uncertainties.

Thus, these results would be in good agreement with the ARPES measurements reported in Ref. 21 if we assume that the 50% smaller gap arises in a third hole pocket, rich in x^2-y^2 orbital content, that is not present in this five-orbital model.

The mean-field calculated spectral functions are shown in Fig. 1(b) along high symmetry directions in the reduced BZ. In the figure, V=0.2 is used[54] and it can be seen that the gaps, that are very similar in magnitude, have opened on all the original FSs. As expected, a numerical inspection of the whole BZ shows that there are no nodes. It can be observed that band distortions and "shadow" (or Bogoliubov) band spectral weight[55] develop only in a small region around the chemical potential.

If a different form factor such as $f(\mathbf{k}) = \cos k_x - \cos k_y$ is considered, the pairing operator would still be purely intraband but with symmetry $B_{1\mathrm{g}}$. While now nodes would appear on the FS because the pairing interaction vanishes for $k_x = \pm k_y$, the gaps on the different FSs still only will differ by the ratio of the form factors at the respective Fermi momenta.

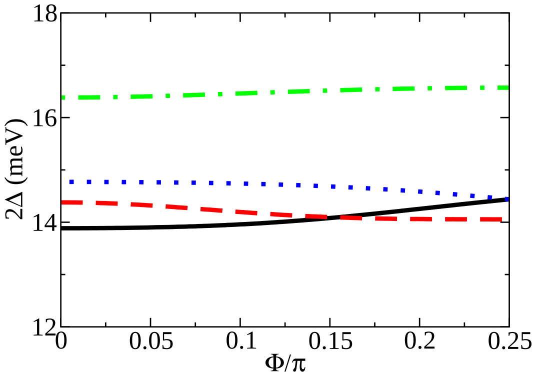

FIG. 2: (Color online) The gap at the internal-hole (dashed-dotted line), external-hole (dashed line), external-electron (continuous line) and internal-electron (dotted line) Fermi surfaces for the $S\pm$ pairing operator with $V = 0.02$. Results are shown as a function of the angle Φ between 0 and $\pi/4$ measured with respect to the k_x axis in counterclockwise [clockwise] direction for the hole [electron (at X)]-pockets. The results are in the folded Brillouin zone.

3. *Multiple Gaps*

Since several experimental[21,23,33,56,57] and theoretical[58,59] efforts have reported the existence of at least two independent gaps at the Fermi surfaces of some pnictides, the next issue to consider is whether there is any other pairing state allowed by symmetry that is purely intraband and able to generate independent gaps in at least one of the FSs. It can be shown that, with the exception of λ_0, all the other 24 λ_i matrices become non-diagonal in the band representation, i.e., $\lambda_i^B = U^{-1}(\mathbf{k})\lambda_i U(\mathbf{k})$ is non-diagonal at least for some values of $\mathbf{k}$ in the BZ. This is true even for λ_i matrices that are diagonal in the orbital representation such as λ_3, λ_8, λ_{23}, and λ_{24}. Thus, *all* these purely intraorbital pairing operators lead to *interband* matrix elements in their band representation. Note that to generate an intraorbital pairing operator that couples electrons in different orbitals with arbitrary strengths we need to consider linear combinations of these diagonal pairing matrices using form factors that provide a well defined symmetry, since we assumed, guided by numerical simulations in models with two and three orbitals, that the pairing operator connects non-degenerate ground states that transform according to one of the one-dimensional irreducible representations of $D_{4\mathrm{h}}$.

We will consider a linear combination of the four intraorbital pairing operators allowed by symmetry that do not require the pairing to be the same in all orbitals. λ_0 is excluded because we already know that it does not produce interband pairing and, thus, it will not contribute to off-diagonal elements in the band representation of the pairing operator. The linear combination to be considered is given by:

$$\Lambda = \alpha_1\lambda_8 f_1(\mathbf{k}) + \alpha_2\lambda_{23} f_2(\mathbf{k}) + \alpha_3\lambda_{24} f_3(\mathbf{k}) + \alpha_4\lambda_3 f_4(\mathbf{k}), \tag{11}$$

where $f_i(\mathbf{k})$ are form factors chosen such that all the terms in Λ transform according to the same irreducible representation. Notice that λ_8, λ_{23}, and λ_{24} transform according to $A_{1\mathrm{g}}$, but λ_3 transforms according to $B_{1\mathrm{g}}$. Thus, for example, a nearest-neighbor pairing operator that transforms according to $A_{1\mathrm{g}}$ will be obtained by setting $f_1(\mathbf{k}) = f_2(\mathbf{k}) = f_3(\mathbf{k}) = \cos k_x + \cos k_y$ and $f_4(\mathbf{k}) = \cos k_x - \cos k_y$. In the band representation Λ becomes

$$\Lambda_b = U^{-1}(\mathbf{k})\Lambda U(\mathbf{k}). \tag{12}$$

If the pairing is purely intraband then Λ_b has to be diagonal. But from the orthogonality properties of U we see that a non-diagonal element $(\Lambda_b)_{i,j}$ can only be zero if $\Lambda_{i,i}$ is the same for all i. However, this is only true for the pairing operator proportional to λ_0 and we have proven numerically that only for $\alpha_j = 0$ in Eq. 11 is $\Lambda_b(m,n) = 0$ for $m \neq n$. Thus, intraorbital pairing with orbital dependent strength leads to interband components of the pairing interaction.[60]

Then, we conclude that if the pairing interaction is purely intraband the pairing mechanism should be associated to a degree of freedom that couples to the five different orbitals with the *same* strength. This means that the gaps in all different FSs must be related, i.e., the symmetry does not allow unrelated gaps in this case. Conversely, if independent gaps are observed on different FSs the symmetry of the highly hybridized orbitals indicates that interband interactions would be present at least in some regions of momentum space, as it will be discussed below.[63]

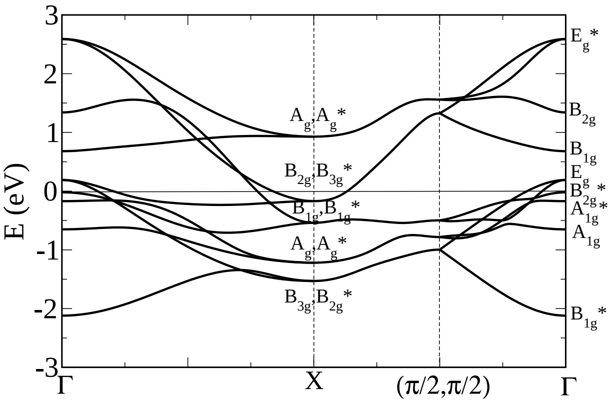

FIG. 3: Band structure of the five-orbital model along high symmetry directions in the reduced Brillouin zone. The irreducible representations of $D_{4\mathrm{h}}(\Gamma)$ and $D_{2\mathrm{h}}(X)$, characterizing the bands at high symmetry points in the reduced BZ, are indicated. For more details see also the discussion in Sec. IV.

Some ARPES data[21] indicate a superconducting state with momentum independent gaps with value Δ at the hole and electron pockets and $\Delta/2$ at a third hole pocket not present in the five-orbital model, at least with the parameters used here and in Ref. 38. However, a slight modification of the parameters, without affecting the symmetry of the Hamiltonian,[64] would create an additional hole pocket around Γ of x^2-y^2 character. This is the state with symmetry $B^*_{2\mathrm{g}}$ at the Γ point shown in Fig. 3. According to this figure, close to the hole FSs around Γ the pairing matrix should be diagonal with elements Δ ($\Delta/2$) for the bands labeled E_{g} ($B^*_{2\mathrm{g}}$) at Γ, which in the unfolded BZ corresponds to *(i)* a diagonal pairing matrix at $\mathbf{k} \approx \mathbf{k}^h_F$ (h denoting the hole Fermi surface) with at least two diagonal elements equal to Δ, and *(ii)* a diagonal pairing matrix at $\mathbf{k} \approx \mathbf{k}^h_F + \mathbf{Q}$ with at least one diagonal element equal to $\Delta/2$. As just discussed, these two different values of a momentum-independent gap cannot arise from purely intraband pairing interactions in a highly hybridized system.

4. Nodeless Gaps with Interband Pairing Matrix Elements

Since several experimental ARPES studies of the pnictides appear to indicate that nodeless gaps open at all the FSs in the superconducting state,[20–24] we will now identify the pairing operators that produce nodeless gaps that are allowed by the symmetries of the five-orbital model.

In a previous study of a three-orbital model we found that, in addition to the $S\pm$ pairing operator, there was another nodeless pairing operator with both intra and interband matrix elements that was called S_{IB}.[39] It leads to intraorbital pairing with different strength for the orbitals xz/yz and xy, and it transforms according to $A_{1\mathrm{g}}$. In the five-orbital model a similar result has been obtained. In fact, we have found several linear combinations with $A_{1\mathrm{g}}$ symmetry of the intraorbital pairing matrices λ_i with $i = 0$, 8, 23, and 24 that provide nodeless gaps. In these pairing states, $f(\mathbf{k}) = 1$ or $\cos k_x \cos k_y$ and the pairing interaction is *not* the same in the different orbitals. The pairing matrix has the form

$$P(\mathbf{k}) = f(\mathbf{k}) \begin{pmatrix} V_1 & 0 & 0 & 0 & 0 \\ 0 & V_1 & 0 & 0 & 0 \\ 0 & 0 & V_2 & 0 & 0 \\ 0 & 0 & 0 & V_3 & 0 \\ 0 & 0 & 0 & 0 & V_4 \end{pmatrix}, \qquad (13)$$

where V_i denote the different pairing strengths. Examples of parameter sets for which nodeless gaps are found are $(V_1, V_1, V_2, V_3, V_4) = V(1, 1, 0, 2, 0)$, $V(1, 1, 0, 1, 0)$, and $V(1, 1, 0, 0, 0)$. These operators pair electrons in the orbitals that contribute the most to the FS, but it is important to notice that they are *not diagonal* in the band representation.

The momentum dependence of the gaps at the FS is shown in Fig. 4(a) for the S_{IB} pairing operator with $f(\mathbf{k}) = \cos k_x \cos k_y$ and $(V_1, V_1, V_2, V_3, V_4) = (0.01, 0.01, 0.0, 0.02, 0.0)/\sqrt{6}$, as special case. To reproduce experimental values for the gap[25] $V = 0.01/\sqrt{6}$ has been chosen. It can be observed that in this case the gaps for the internal hole and electron pockets in panel (a) (dashed-dotted and dotted lines) have a negligible momentum dependence and an average value of about 5 meV. The external hole pocket has a smaller gap, about 3.5 meV, with a very weak momentum dependence (dashed line). The strongest dependence with momentum occurs in the external electron pocket (continuous line) with the gap reaching a value of about 7.5 meV at the point along the x-axis where the electron pocket is the closest to the hole pockets and has pure xy orbital character. As the point where the two electron-like FSs intersect each other ($\Phi = \pi/4$) is approached, the external electron-pocket acquires xz/yz character and the magnitude of the gap converges to the almost momentum independent value of 5 meV that characterizes the internal electron-pocket. Thus, this is a case in which a direct measurement of the gaps would indicate the presence of three “independent” gaps. The gaps in the internal electron and hole pockets behave as expected in the $S\pm$ pairing scenario,[49–53] while the external hole and electron pockets show a different gap value. While this would agree with experimental results that favor multiple gaps[21,23,33,56–59] it is important to realize that this pairing operator contains interband matrix elements that must be incorporated in the description of a possible pairing mechanism.

Modifying V_i we can tune the relative gap values, obtaining three almost momentum independent gaps with values 3.5 meV, 5.5 meV, and 7.5 meV (in the external-hole, internal-hole, and internal-electron pockets, respectively) as shown in Fig. 4(b). In addition, a gap with

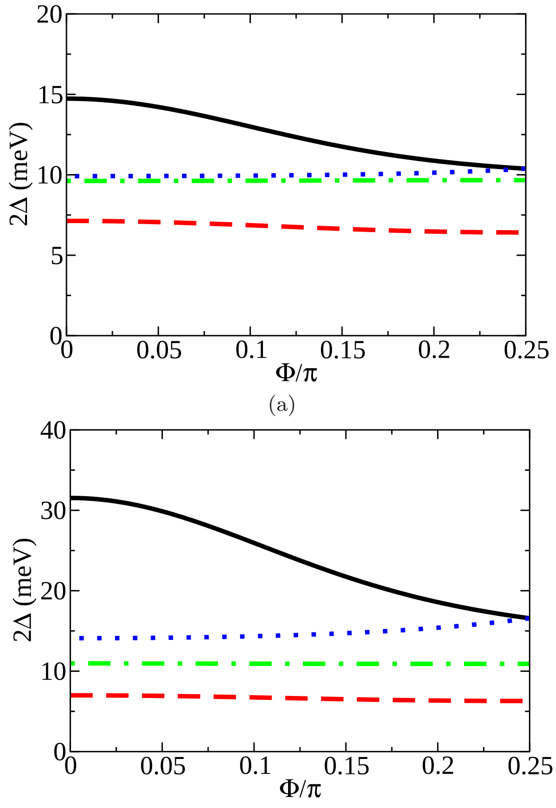

(a)

(b)

FIG. 4: (Color online) The gap at the internal-hole (dashed-dotted line), external-hole (dashed line), external-electron (continuous line), and internal-electron (dotted line) Fermi surfaces for the nodeless pairing operator $S_{\rm IB}$ with (a) $(V_1, V_1, V_2, V_3, V_4) = (0.01, 0.01, 0.0, 0.02, 0.0)/\sqrt{6}$ and (b) $(V_1, V_1, V_2, V_3, V_4) = (0.005, 0.005, 0.0, 0.02, 0.0)$. Results are shown as a function of the angle Φ between 0 and $\pi/4$ measured with respect to the k_x axis in counterclockwise (clockwise) direction for the hole [electron (at X)]-pockets. The notation is as in Fig. 2.

momentum dependence ranging between 15 meV and 7.5 meV appears at the external electron pocket which has the largest xy contribution. Thus, this interaction would lead to four apparently independent nodeless gaps.

B. Interorbital Pairing Operators

As discussed above, due to the strong hybridization of all five d orbitals we have verified that all the intraorbital pairing operators allowed by the lattice and orbital symmetries of the pnictides lead to interband pairing interactions if $\lambda_i \neq \lambda_0$. Interband pairing has always been considered unlikely in BCS theory[46] because the pairing attraction acts in a very narrow energy range around the FS. However, in a system in which two FSs formed by different bands are very close to each other (e.g. the two hole pockets in the pnictides that cannot be distinguished in ARPES experiments,[21,23,24] or the two electron pockets that intersect at two points) then the formation of interband pairs, as it was described in Ref. 47, could occur. In addition, numerical Lanczos studies of a two-orbital model for the pnictides suggest that an interorbital pairing state with B_{2g} symmetry, with interband components, could be the favored pairing state in the intermediate Hubbard U regime.[40–42] For this reason, here results will be presented for some interorbital pairing operators that have interband attraction, at least in some regions of the BZ. The effects of this interaction will be addressed later in Sec. IV.

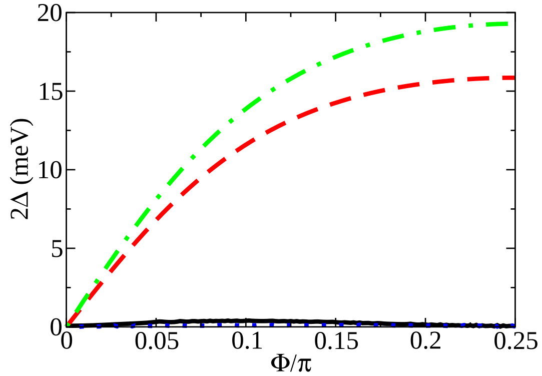

FIG. 5: (Color online) The gap at the internal-hole (dashed-dotted line), external-hole (dashed line), external-electron (continuous line), and internal-electron (dotted line) Fermi surfaces for the interorbital pairing operator B_{2g} with $V = 0.012/\sqrt{5}$. Results are shown as a function of the angle Φ between 0 and $\pi/4$ measured with respect to the k_x axis in counterclockwise [clockwise] direction for the hole [electron (at X)]-pockets. The notation is as in Fig. 2

.

First let us consider the B_{2g} pairing operator mentioned in the previous paragraph. It is given by

$$\Delta^{\dagger}_{B_{2g}}(\mathbf{k}) = V(\cos k_x + \cos k_y) \sum_{\alpha\neq\beta=1}^{2} d^{\dagger}_{\mathbf{k},\alpha,\uparrow} d^{\dagger}_{-\mathbf{k},\beta,\downarrow}. \quad (14)$$

For this operator, the structure of the gap strongly depends on the value of the pairing attraction V. For values of V compatible with the order of magnitude of the gaps reported from experiments in the pnictides, which are of the order of meV, the behavior of the gap at the different FSs is shown in Fig. 5. The gap on the two hole pockets presents nodes along the x ($\Phi = 0$) and y ($\Phi = \pi/2$) axes (the latter not shown explicitly since the results are symmetric and thus $\Delta(\Phi) = \Delta(\pi/2 - \Phi)$). Both gaps are maximized along the diagonal direction ($\Phi = \pi/4$). Thus, it would resemble "d_{xy}-wave" behavior in experiments where only the node location but not the phase of the gap can be measured. The reason for the existence of the nodes is that along the x and y axes the pairing interaction is purely interorbital, but V is not strong enough to open a gap (a finite value of V is needed to open a gap with purely interorbital pairing, as discussed in previous literature[47]) and that effect creates the node. By contrast, in Fig. 6(a) we show the mean-field calculated spectral functions along some high symmetry directions of the reduced BZ for the same pairing operator but with a larger $V = 0.2$. In this case, the gaps have opened on the hole-pocket FSs around the Γ point. But for this value of V the gap is of the order of 100 meV, i.e. too large compared with the experimental results for the pnictides.

Another characteristic of the $B_{2\mathrm{g}}$ pairing operator is that the gap in the electron pockets presents nodes along the x and y axes (for the same reason than the hole pockets at weak V) but also at the points where the two electron pockets cross, $\Phi = \pi/4$, because $f(\mathbf{k}) = 0$ there. For $V < 0.01$ the gap is much smaller than the one on the hole-pockets, as shown in Fig. 5. As V increases, a gap opens along the x and y axes for the internal electron pocket, as it can be observed in Fig. 6(a) for $V = 0.2$. However, in this case nodes remain along these axes for the external electron pocket. The reason is that at these points the FS arises from bands that have mostly character xz/xy or yz/xy[38] and, thus, the operator $\Delta^{\dagger}_{B_{2g}}$, which couples electrons in the xz/yz orbitals, is not effective at opening a gap along the momentum axis where one of the FSs has purely xy character. While this gap structure for the $B_{2\mathrm{g}}$ pairing state disagrees with ARPES measurements it is important to keep in mind that the existence of nodes in some pnictides has been reported by several groups using other experimental techniques. Thus, it is still possible that the surface that is actually tested by ARPES does not present the same behavior as the bulk in the pnictides.

A natural generalization of the operator $\Delta^{\dagger}_{B_{2\mathrm{g}}}$ to include the xy orbital was provided in Ref. 39. The extended operator is a linear combination of $\Delta^{\dagger}_{B_{2\mathrm{g}}}$ (Eq. 14) and

$$\Delta^{\dagger}_{V_g}(\mathbf{k}) = V'[\sin k_x \sum_{\alpha\neq\beta=2,4} d^{\dagger}_{\mathbf{k},\alpha,\uparrow} d^{\dagger}_{-\mathbf{k},\beta,\downarrow} - \sin k_y \sum_{\alpha\neq\beta=1,4} d^{\dagger}_{\mathbf{k},\alpha,\uparrow} d^{\dagger}_{-\mathbf{k},\beta,\downarrow}]. \qquad (15)$$

The total pairing operator has symmetry $B_{2\mathrm{g}}$. Note that now the 10×10 matrix given in Eq. 4 will provide pairs with pseudocrystal momentum 0 for the particles in orbitals 1 and 2, but $\mathbf{Q}$ for one of the particles in orbital 4 and the other in 1 or 2. Thus, we must consider the 20×20 BdG matrix mentioned earlier and we have studied the extended $B_{2\mathrm{g}}$ pairing with the two possible pseudocrystal momenta 0 and $\mathbf{Q}$. This generalized form removes the nodes at the crossing point of the two electron pockets, since $\Delta^{\dagger}_{V_g}$ is finite at those points.

In Fig. 6(b) we show the spectral function for $V = V' = 0.2$ for pairs with 0 pseudocrystal momentum. It can be seen that isolated nodes at the electron pockets remain only at the points along the momentum axis where they have purely xy character. However, for smaller values of $V = V'$ that produce gaps in the meV range, we have found that nodes along the axis remain and the gaps resemble very much those obtained with the original $B_{2\mathrm{g}}$ pairing operator shown in Fig. 5.

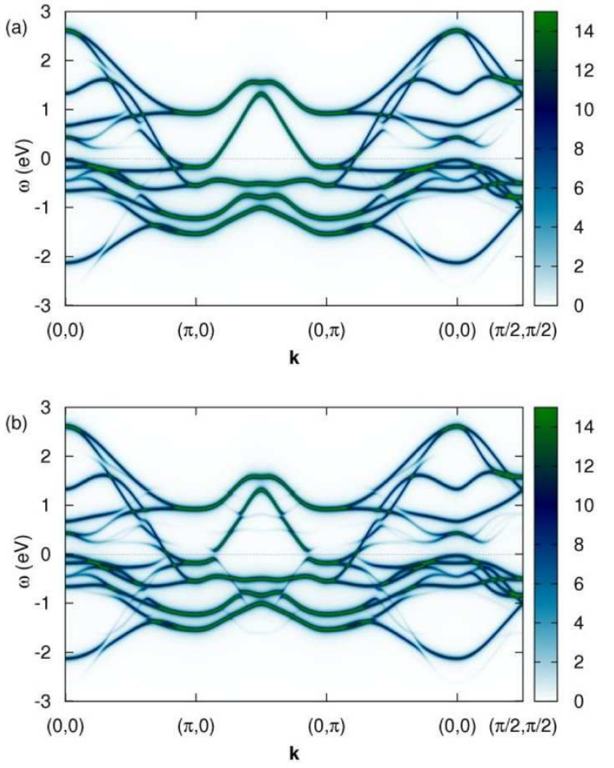

FIG. 6: (Color online) The intensity of the points represent the values of the spectral function $A(\mathbf{k},\omega)$ for the five-orbital model with pairing interaction $V = 0.2$, for the pairing operator (a) $B_{2\mathrm{g}}$ and (b) extended $B_{2\mathrm{g}}$ discussed in the text. The results are shown in the reduced BZ.

IV. DISCUSSION

In theoretical studies of multiorbital systems it has been "traditional" to consider non-hybridized orbitals/bands.[46] While this approach works for simple cases, in the pnictides the hybridization of the orbitals is strong.[14,15] As a result, the energies in the band representation $\epsilon_j(\mathbf{k})$ have several accidental degeneracies within the Brillouin Zone which means that the bands cross at several points and are, thus, very entangled.[65] This band entanglement is apparent in Fig. 3, where the eigenvalues of H_{TB} are shown along high symmetry directions in the folded BZ. The irreducible representations characterizing the bands at some high symmetry points (such as Γ with symmetry $D_{4\mathrm{h}}$ and X with symmetry $D_{2\mathrm{h}}$) are indicated, and the star labels bands determined by states with pseudocrystal momentum $\mathbf{k}+\mathbf{Q}$. For example, the band labeled B_{1g} at Γ, crosses two other bands along the $\Gamma - X$ direction. Thus, the approach used in early studies by Suhl *et al.*, where a gap Δ_j is associated to a band with energy $\epsilon_j(\mathbf{k})$ in all the BZ, becomes ambiguous in this case. In a system with strongly hybridized orbitals, it is more reasonable to define pairing operators in the orbital representation because the orbital basis is globally well-defined at all points in the BZ, while the band assignation is local. In addition, as it was shown in the previous Section, the orbital representation provides the natural framework to construct the pairing operators that are allowed by symmetry. All the active degrees of freedom need to be incorporated in the pairing operators since otherwise the results can be misleading, as in the early studies of magnetization when the contribution of the spin to the spatial wave function was disregarded. Then, when intraband pairing operators are constructed their orbital content should be provided.

Another important point is to understand the consequences of interband matrix elements arising from the symmetry of the pairing operators. As shown in Ref. 47, at points in the BZ where there are intra and interband elements in $P_{\rm B}(\mathbf{k})$ the pairs will be formed by electrons in the same band if the pairing interaction is weak or intermediate, which seems to be the case in the pnictides. It is only at the very few points on the FS where $P_{\rm B}(\mathbf{k})$ has finite (zero) non-diagonal (diagonal) elements that the pairing attraction will be purely interband. At these points, if the pairing attraction is weak we would expect to observe nodes.[47] It is only when the two FS are very close (as for the two almost degenerate hole pockets), and when the pairing interaction is strong enough, that interband pairs would be possible.[47]

As pointed out in the Introduction, the properties of the pairing operator in the pnictides have not been established yet and data obtained with different experimental techniques are in disagreement. ARPES results are interpreted as indicative of nodeless gaps with at most a very weak momentum dependence. Some groups have identified gaps with the same magnitude in the electron and one of the hole pockets,[20–24] while others have found them to be different.[25] In addition, the gap in a third hole pocket, not of xz/yz character, is found to be different from the gap in the electron pockets and, thus, the existence of two and, even three, gaps in these materials has been proposed. The symmetry arguments presented here indicate that truly momentum independent gaps would have to be equal (including the sign of the order parameter) in all Fermi surfaces. If a momentum dependence is allowed, then a pairing state such as the $S\pm$ could arise. In this case the gap in the hole and electron pockets related by nesting should be very similar (although with opposite signs in the order parameters) and the gap in the additional hole pocket would differ only by the ratio between the form factors $f(\mathbf{k})$ at the locations of the two different hole-pockets. Thus, there should be only one gap in the sense that the coupling between the electrons and the interaction causing the pairing will not be orbital dependent and the band dependence is only due to the different Fermi momenta.

We have also shown that a pairing interaction that couples with an orbital-dependent strength to the electrons leads to a pairing matrix that is not diagonal in the band representation. Some of these operators open weakly momentum dependent nodeless gaps in the different FSs. While this kind of pairing operator could agree with some experimental results, it would be necessary to take into account the interband pairing interactions when developing the associated microscopic pairing mechanism.

Note that the existence of nodes in the pnictides is in fact supported by transport experiments,[26–36] in clear contradiction with ARPES. Thus, more experimental work is needed in order to clarify this issue. We have found a large variety of nodal pairing operators that respect the symmetry of the pnictides: this includes those proportional to the identity in the orbital sector, with their nodes arising from the zeroes in $f(\mathbf{k})$, and also other pairing operators in which electrons in different orbitals are subject to different pairing strengths and, thus, give rise to interband terms in the pairing matrices.

The $S\pm$ pairing operator with symmetry A_{1g} appears to be the favored one in the literature,[49–53] but numerical calculations in a two-orbital model[40,41] while indicating that this pairing prevails in strong coupling, lead in the intermediate regime to a pairing state made of electrons in different orbitals and with symmetry B_{2g}. Since the orbitals xz and yz are strongly hybridized forming the bands that produce the hole pockets, this kind of pairing could be possible. If realized, it would induce nodes on the hole and electron pockets and the pair formation would be much stronger in the hole than in the electron pockets. Interestingly, the gaps in the two hole pockets would be different (see Fig. 5) which may be in agreement with some of the experimental results that indicate two nodal gaps.[67]

V. CONCLUSIONS

Summarizing, we have shown that in a model that retains the symmetry of the FeAs planes for the pnictides and considers the five d orbitals of the Fe ions, a purely intraband pairing operator can only result from an intraorbital pairing interaction that affects electrons in the different orbitals with *identical strength.* In this case, the symmetry of the pairing operator is entirely determined by the form factor $f(\mathbf{k})$ which depends only on the spatial location of the particles that form the pairs. As a result, gaps in different portions of the FS can differ only by the ratios of the form factors, i.e., two or more unrelated gaps *cannot* occur. Conversely, multiple gaps as observed experimentally, or orbital dependent pairing attractions, would indicate interband pairing interactions at least in some regions of the BZ. Then, this feature should be incorporated in theoretical proposals for the pairing mechanism. If there are special points in the BZ where the attraction is purely interband, then nodes or interband pairing will occur depending on whether the interaction is weak or strong. Experimental measurements of the gap magnitude indicate that the pairing attraction is weak, thus nodes rather than interband pairing would be expected.

The present analysis suggests that if the pairing mechanism is purely intraband, as assumed by many, then no unrelated gaps should occur in the different portions of the FS. Reciprocally, if it is experimentally confirmed the existence of two or more unrelated gaps this would point to the need to consider interband, in addition to intraband, pairing interactions in any realistic microscopic description of the pairing mechanism.

VI. ACKNOWLEDGMENTS

This work was supported by the National Science Foundation grant DMR-0706020 and by the Division of Materials Sciences and Engineering, Office of Basic Energy Sciences, U.S. Department of Energy, M. D. acknowledges partial suppost from the DFG under the Emmy-Noether program.

Appendix A: Expressions for the Tight Binding Hamiltonian

$$
\begin{aligned}
\xi_{11} &= 2t_x^{11}\cos k_x + 2t_y^{11}\cos k_y + 4t_{xy}^{11}\cos k_x\cos k_y + \\
&\quad 2t_{xx}^{11}(\cos 2k_x - \cos 2k_y) + 4t_{xxy}^{11}\cos 2k_x\cos k_y \\
&\quad +4t_{xyy}^{11}\cos 2k_y\cos k_x + 4t_{xxyy}^{11}\cos 2k_x\cos 2k_y \qquad \text{(A1)}\\
\xi_{22} &= 2t_y^{11}\cos k_x + 2t_x^{11}\cos k_y + 4t_{xy}^{11}\cos k_x\cos k_y - \\
&\quad 2t_{xx}^{11}(\cos 2k_x - \cos 2k_y) + 4t_{xyy}^{11}\cos 2k_x\cos k_y \\
&\quad +4t_{xxy}^{11}\cos 2k_y\cos k_x + 4t_{xxyy}^{11}\cos 2k_x\cos 2k_y \qquad \text{(A2)}\\
\xi_{33} &= 2t_x^{33}(\cos k_x + \cos k_y) + 4t_{xy}^{33}\cos k_x\cos k_y + \\
&\quad 2t_{xx}^{33}(\cos 2k_x + \cos 2k_y) \qquad \text{(A3)}\\
\xi_{44} &= 2t_x^{44}(\cos k_x + \cos k_y) + 4t_{xy}^{44}\cos k_x\cos k_y + \\
&\quad 2t_{xx}^{44}(\cos 2k_x + \cos 2k_y) \\
&\quad +4t_{xxy}^{44}(\cos 2k_x\cos k_y + \cos 2k_y\cos k_x) + \\
&\quad 4t_{xxyy}^{44}\cos 2k_x\cos 2k_y \qquad \text{(A4)}\\
\xi_{55} &= 2t_x^{55}(\cos k_x + \cos k_y) + 2t_{xx}^{55}(\cos 2k_x + \cos 2k_y) + \\
&\quad 4t_{xxy}^{55}(\cos 2k_x\cos k_y + \cos 2k_y\cos k_x) \\
&\quad +4t_{xxyy}^{55}\cos 2k_x\cos 2k_y \qquad \text{(A5)}\\
\xi_{12} &= 4t_{xy}^{12}\sin k_x\sin k_y + \\
&\quad 4t_{xxy}^{12}(\sin 2k_x\sin k_y + \sin 2k_y\sin k_x) + \\
&\quad 4t_{xxyy}^{12}\sin 2k_x\sin 2k_y \qquad \text{(A6)}\\
\xi_{13} &= 2it_x^{13}\sin k_y + 4it_{xy}^{13}\sin k_y\cos k_x - \\
&\quad 4it_{xxy}^{13}(\sin 2k_y\cos k_x - \cos 2k_x\sin k_y) \qquad \text{(A7)}\\
\xi_{23} &= 2it_x^{13}\sin k_x + 4it_{xy}^{13}\sin k_x\cos k_y - \\
&\quad 4it_{xxy}^{13}(\sin 2k_x\cos k_y - \cos 2k_y\sin k_x) \qquad \text{(A8)}\\
\xi_{14} &= 2it_x^{14}\sin k_x + 4it_{xy}^{14}\cos k_y\sin k_x + \\
&\quad 4it_{xxy}^{14}\sin 2k_x\cos k_y \qquad \text{(A9)}\\
\xi_{24} &= -2it_x^{14}\sin k_y + 4it_{xy}^{14}\cos k_x\sin k_y - \\
&\quad 4it_{xxy}^{14}\sin 2k_y\cos k_x \qquad \text{(A10)}\\
\xi_{15} &= 2it_x^{15}\sin k_y - 4it_{xy}^{15}\sin k_y\cos k_x \\
&\quad -4it_{xxyy}^{15}\sin 2k_y\cos 2k_x \qquad \text{(A11)}\\
\xi_{25} &= -2it_x^{15}\sin k_x + 4it_{xy}^{15}\sin k_x\cos k_y \\
&\quad +4it_{xxyy}^{15}\sin 2k_x\cos 2k_y \qquad \text{(A12)}\\
\xi_{34} &= 4t_{xxy}^{34}(\sin 2k_y\sin k_x - \sin 2k_x\sin k_y) \qquad \text{(A13)}\\
\xi_{35} &= 2t_x^{35}(\cos k_x - \cos k_y) + \\
&\quad 4t_{xxy}^{35}(\cos 2k_x\cos k_y - \cos 2k_y\cos k_x) \qquad \text{(A14)}\\
\xi_{45} &= 4t_{xy}^{45}\sin k_x\sin k_y + 4t_{xxyy}^{45}\sin 2k_x\sin 2k_y \qquad \text{(A15)}
\end{aligned}
$$

The values of the hopping parameters t_α^{ij} are explicitly provided in Ref. 38.

---

[1] Y. Kamihara, T. Watanabe, M. Hirano, and H. Hosono, J. Am. Chem. Soc **130**, 3296 (2008).

[2] G. F. Chen, Z. Li, G. Li, J. Zhou, D. Wu, J. Dong, W. Z. Hu, P. Zheng, Z. J. Chen, H. Q. Yuan, J. Singleton, J. L. Luo, and N. L. Wang, Phys. Rev. Lett. **101**, 057007 (2008).

[3] G. F. Chen, Z. Li, D. Wu, G. Li, W. Z. Hu, J. Dong, P. Zheng, J. L. Luo, and N. L. Wang, Phys. Rev. Lett. **100**, 247002 (2008).

[4] H.-H. Wen, G. Mu, L. Fang, H. Yang, and X. Zhu, EPL **82**, 17009 (2008).

[5] X. H. Chen, T. Wu, G. Wu, R. H. Liu, H. Chen, and D. F. Fang, Nature **453**, 761 (2008).

[6] Z. Ren, J. Yang, W. Lu, W. Yi, G. Che, X. Dong, L. Sun, and Z. Zhao, Mater. Res. Innovat. **12**, 105 (2008).

[7] Z.-A. Ren, W. Lu, J. Yang, W. Yi, X.-L. Shen, Z.-C. Li, G.-C. Che, X.-L. Dong, L.-L. Sun, F. Zhou, and Z.-X. Zhao, Chin. Phys. Lett. **25**, 2215 (2008).

[8] Z.-A. Ren, W. Lu, J. Yang, W. Yi, X.-L. Shen, Z.-C. Li, G.-C. Che, X.-L.Dong, L.-L. Sun, F. Zhou, and Z.-X. Zhao, EPL **83**, 17002 (2008).

[9] J. Dong, H. J. Zhang, G. Xu, Z. Li, G. Li, W. Z. Hu, D. Wu, G. F. Chen, X. Dai, J. L. Luo, Z. Fang, and N. L. Wang, EPL **83**, 27006 (2008).

[10] C. de la Cruz, Q. Huang, J. W. Lynn, J. Li, W. Ratcliff II, J. L. Zarestky, H. A. Mook, G. F. Chen, J. L. Luo, N. L. Wang, and P. Dai, Nature **453**, 899 (2008).

[11] Y. Chen, J. W. Lynn, J. Li, G. Li, G. F. Chen, J. L. Luo, N. L. Wang, P. Dai, C. de la Cruz, and H. A. Mook, Phys.

Rev. B **78**, 064515 (2008).

[12] C. Krellner, N. Caroca-Canales, A. Jesche, H. Rosner, A. Ormeci, and C. Geibel, Phys. Rev. B **78**, 100504 (2008).

[13] A. I. Goldman, D. N. Argyriou, B. Ouladdiaf, T. Chatterji, A. Kreyssig, S. Nandi, N. Ni, S. L. Bud'ko, P. C. Canfield, and R. J. McQueeney, Phys. Rev. B **78**, 100506 (2008).

[14] L. Boeri, O. V. Dolgov, and A. A. Golubov, Phys. Rev. Lett. **101**, 026403 (2008).

[15] S. Lebegue, Phys. Rev. B **75**, 035110 (2007).

[16] G. Xu, W. Ming, Y. Yao, X. Dai, S.-C. Zhang, and Z. Fang, EPL **82**, 67002 (2008).

[17] C. Cao, P. J. Hirschfeld, and H.-P. Cheng, Phys. Rev. B **77**, 220506 (2008).

[18] H.-J. Zhang, G. Xu, X. Dai, and Z. Fang, Chin. Phys. Lett. **26**, 017401 (2009).

[19] E. Dagotto, Rev. Mod. Phys. **66**, 763 (1994).

[20] T. Kondo, A. F. Santander-Syro, O. Copie, C. Liu, M. E. Tillman, E. D. Mun, J. Schmalian, S. L. Bud'ko, M. A. Tanatar, P. C. Canfield, and A. Kaminski, Phys. Rev. Lett. **101**, 147003 (2008).

[21] H. Ding, P. Richard, K. Nakayama, K. Sugawara, T. Arakane, Y. Sekiba, A. Takayama, S. Souma, T. Sato, T. Takahashi, Z. Wang, X. Dai, Z. Fang, G. F. Chen, J. L. Luo, and N. L. Wang, EPL **83**, 47001 (2008).

[22] K. Nakayama, T. Sato, P. Richard, Y.-M. Xu, Y. Sekiba, S. Souma, G. F. Chen, J. L. Luo, N. L. Wang, H. Ding, T. Takahashi, EPL **85**, 67002 (2009).

[23] L. Wray, D. Qian, D. Hsieh, Y. Xia, L. Li, J.G. Checkelsky, A. Pasupathy, K.K. Gomes, A.V. Fedorov, G.F. Chen, J.L. Luo, A. Yazdani, N.P. Ong, N.L. Wang, M.Z. Hasan, arXiv:0808.2185.

[24] D. Hsieh, Y. Xia, L. Wray, D. Qian, K. Gomes, A. Yazdani, G.F. Chen, J.L. Luo, N.L. Wang, and M.Z.Hasan, arXiv:0812.2289 (2008).

[25] K.W. Kim, M. Röslle, A. Dubroka, V.K. Malik, T. Wolf, and C. Bernhard, arXiv:0912.0140.

[26] L. Shan, Y. Wang, X. Zhu, G. Mu, L. Fang, C. Ren, and H.-H. Wen, EPL **83**, 57004 (2008).

[27] M. Gang, Z. Xi-Yu, F. Lei, S. Lei, R. Cong, and W. Hai-Hu, Chin. Phys. Lett. **25**, 2221 (2008).

[28] C. Ren, Z.-S. Wang, H. Yang, X. Zhu, L. Fang, G. Mu, L. Shan, and H.-H. Wen, arXiv:0804.1726, 2008.

[29] K. Ahilan, F. L. Ning, T. Imai, A. S. Sefat, R. Jin, M. A. McGuire, B. C. Sales, and D. Mandrus, Phys. Rev. B **78**, 100501 (2008).

[30] Y. Nakai, K. Ishida, Y. Kamihara, M. Hirano, and H. Hosono, J. Phys. Soc. Jpn. **77**, 073701 (2008).

[31] H.-J. Grafe, D. Paar, G. Lang, N. J. Curro, G. Behr, J. Werner, J. Hamann-Borrero, C. Hess, N. Leps, R. Klingeler, and B. Büchner, Phys. Rev. Lett. **101**, 047003 (2008).

[32] Y.-L. Wang, L. Shan, L. Fang, P. Cheng, C. Ren, and H.-H. Wen, Supercond. Sci. Technol. **22**, 015018 (2009).

[33] K. Matano, Z. A. Ren, X. L. Dong, L. L. Sun, Z. X. Zhao, and G. qing Zheng, EPL **83**, 57001 (2008).

[34] H. Mukuda, N. Terasaki, H. Kinouchi, M. Yashima, Y. Kitaoka, S. Suzuki, S. Miyasaka, S. Tajima, K. Miyazawa, P. Shirage, H. Kito, H. Eisaki, and A. Iyo, J. Phys. Soc. Jpn. **77**, 093704 (2008).

[35] O. Millo, I. Asulin, O. Yuli, I. Felner, Z.-A. Ren, X.-L. Shen, G.-C. Che, and Z.-X. Zhao, Phys. Rev. B **78**, 092505 (2008).

[36] X. L. Wang, S. X. Dou, Z.-A. Ren, W. Yi, Z.-C. Li, Z.-X. Zhao, and S.-I. Lee, J. Phys.: Condens. Matter **21**, 205701 (2009).2008.

[37] V. Mishra, G. Boyd, S. Graser, T. Maier, P.J. Hirschfeld, and D.J. Scalapino, arXiv:0901.2653.

[38] S. Graser, T.A. Maier, P.J. Hirschfeld, and D.J. Scalapino, New J. Phys. **11**, 025016 (2009).

[39] M. Daghofer, A. Moreo, A. Nicholson, and E. Dagotto, Phys. Rev. B.**81**, 014511 (2010).

[40] M. Daghofer, A. Moreo, J. A. Riera, E. Arrigoni, D. J. Scalapino, and E. Dagotto, Phys. Rev. Lett. **101**, 237004 (2008).

[41] A. Moreo, M. Daghofer, J. A. Riera, and E. Dagotto, Phys. Rev. B **79**, 134502 (2009).

[42] R. Yu, K. T. Trinh, A. Moreo, M. Daghofer, J. Riera, S. Haas, and E. Dagotto, Phys. Rev. B **79**, 104510 (2009).

[43] H. Eschrig and K. Koepernik, Phys. Rev. B **80**, 104503 (2009).

[44] Y. Zhou, W.-Q. Chen, and F.-C. Zhang, Phys. Rev. B **78**, 064514 (2008).

[45] Y. Wan and Q.-H. Wang, EPL **85**, 57007 (2009).

[46] H. Suhl, B. T. Matthias, and L. R. Walker, Phys. Rev. Lett. **3**, 552 (1959).

[47] A. Moreo, M. Daghofer, A. Nicholson, and E. Dagotto, Phys. Rev. B **80**, 104507 (2009).

[48] Notice that a pair with pseudocrystal momentum **Q** still has crystal momentum zero.[39]

[49] K. Kuroki, S. Onari, R. Arita, H. Usui, Y. Tanaka, H. Kontani, and H. Aoki, Phys. Rev. Lett. **101**, 087004 (2008).

[50] I. Mazin, D. Singh, M. Johannes, and M. Du, Phys. Rev. Lett. **101**, 057003 (2008).

[51] M. M. Korshunov and I. Eremin, Phys. Rev. B **78**, 140509 (2008).

[52] D. Parker, O. V. Dolgov, M. M. Korshunov, A. A. Golubov, and I. I. Mazin, Phys. Rev. B **78**, 134524 (2008).

[53] K. Seo, A.B. Bernevig and J.P. Hu, Phys. Rev. Lett. **101**, 206404 (2008); M.M. Parish, J.P. Hu, and B.A. Bernevig, Phys. Rev. B **78**, 144514 (2008).

[54] The value of V has been chosen so that the gaps can be seen in a scale where the whole bandwidth range is displayed.

[55] S. Haas, A. Moreo, and E. Dagotto, Phys. Rev. Lett. **74**, 4281 (1995). contains a discussion and references on shadow bands in the context of the cuprates.

[56] P. Szabo, Z. Pribulova, G. Pristas, S.L. Bud'ko, P.C. Canfield, and P. Samuely, Physica **B404**, 3220 (2009) and Phys. Rev. B **79**, 012503 (2009).

[57] B. Muschler, W. Prestel, R. Hackl, T. P. Devereaux, J. G. Analytis, Jiun-Haw Chu, and I. R. Fisher, arXiv:0910.0898.

[58] V. Stanev, J. Kang, and Z. Tesanovic, Phys. Rev. B **78**, 184509 (2008).

[59] G. R. Boyd, T. P. Devereaux, P. J. Hirschfeld, V. Mishra, and D. J. Scalapino, Phys. Rev. B **79**, 174521 (2009).

[60] The five-orbital model being considered here has strong hybridization among the five orbitals and, as a result, the change of basis matrix U does not have a block diagonal structure for all values of the momentum. If this were the case, it would be possible to obtain a pure intraband pairing arising from intraorbital pairing with orbital dependent strength. Orbitals that do not hybridize with each other could have different pairing strengths, which in turn may produce FSs with independent gapas it is the case in MgB$_2$[61] and NdSe$_2$[62].

[61] Hyoung Joon Choi, David Roundy, Hong Sun, Marvin L. Cohen, and Steven G. Louie, Nature (London) 418, 758 (2002), and references therein.

[62] Etienne Boaknin, M. A. Tanatar, Johnpierre Paglione, D. Hawthorn, F. Ronning, R. W. Hill, M. Sutherland, Louis Taillefer, Jeff Sonier, S. M. Hayden, and J. W. Brill, Phys. Rev. Lett. **90**, 117003 (2003).

[63] Notice that linear combinations of form factors that create pairs of different sizes would be allowed by symmetry considerations. However, since the spatial extension of the pairs can be determined from experiments, we consider in this work pairing operators that create pairs of a fixed size as given in Eq. 3.

[64] M. J. Calderon, B. Valenzuela, E. Bascones, Phys. Rev. **B** 80, 094531 (2009).

[65] This actually results from the symmetry of the pnictides since among the four structural families constituting the iron-based superconducting pnictides the 11, 111, and 1111 are characterized by a nonsymmorphic space group.[43] In this kind of systems all energy bands corresponding to elementary band representations are necessarily composite and connected.[66]

[66] L. Michel and J. Zac, EPL **50**, 519 (2000); L. Michel and J. Zac, Phys. Rev. B **59**, 5998 (1999).

[67] F. Hardy, T. Wolf, R.A. Fisher, R.Eder, P. Schweiss, P. Adelmann, H. V. Löehneysen, C. Meingast, Phys. Rev. B **81**, 060501(R) (2010); K. Gofryk, A.S. Sefat, E.D. Bauer, M.A. McGuire, B.C. Sales, D. Mandrus, J.D. Thompson, and F. Ronning, New J. Phys. **12** 023006 (2010).